

We are IntechOpen, the world's leading publisher of Open Access books Built by scientists, for scientists

4,200

Open access books available

116,000

International authors and editors

125M

Downloads

Our authors are among the

154

Countries delivered to

TOP 1%

most cited scientists

12.2%

Contributors from top 500 universities



WEB OF SCIENCE™

Selection of our books indexed in the Book Citation Index
in Web of Science™ Core Collection (BKCI)

Interested in publishing with us?
Contact book.department@intechopen.com

Numbers displayed above are based on latest data collected.
For more information visit www.intechopen.com



Study of Heat Dissipation Mechanism in Nanoscale MOSFETs Using BDE Model

Housseem Rezgui, Faouzi Nasri,
Mohamed Fadhel Ben Aissa and
Amen Allah Guizani

Additional information is available at the end of the chapter

<http://dx.doi.org/10.5772/intechopen.75595>

Abstract

In this chapter, we report the nano-heat transport in metal-oxide-semiconductor field effect transistor (MOSFET). We propose a ballistic-diffusive model (BDE) to inquire the thermal stability of nanoscale MOSFET's. To study the mechanism of scattering in the interface oxide-semiconductor, we have included the specular parameter defined as the probability of reflection at boundary. In addition, we have studied the effective thermal conductivity (ETC) in nanofilms we found that ETC depend with the size of nanomaterial. The finite element method (FEM) is used to resolve the results for a 10 nm channel length. The results prove that our proposed model is close to those results obtained by the Boltzmann transport equation (BTE).

Keywords: nano-devices, thermal conductivity, BDE model, temperature jump, heat dissipation

1. Introduction

Considerable exploration focused on the fast progress of nanodevice. In recent years, the thermal analysis is important to inquire the phonon transport in nano-materials. The study of the heat conduction in nano-electronics lead to compare the thermal stability of nano-transistors [1–3]. The increase of the heat dissipation has been owned by the miniaturization and the reduction of the thermal conductivity [3]. The smaller channel device was assumed to

(13) nm for the current (2018) and less than (6) nm for long-term (2026) [4]. The Fourier's law has generally used to predict the diffusive heat conduction [5]. In nanoscale the characteristic time and size of nanodevice was smaller than the mean free path (MFP). The classical heat conduction based on local equilibrium lead to the linear equation

$$q = -\kappa \nabla T \quad (1)$$

where q is the heat flux, ∇T is the temperature gradient and κ is the bulk thermal conductivity. Actually, the BTE is an effective method to study the non-continuous temperature and heat flux in nanosystems [6, 7]. Many transport models have been derived from the BTE used to investigate the thermal transport in solid interface [8], nano-transistor [9–12] and carbon nanotubes [13].

Alvarez et al. [14] have studied the nonlocal effect in nanoscale devices. They inquired the heat transport in ballistic regime. They found that the thermal conductivity bank on the Knudsen number.

Nano-heat transport includes both temporal aspects and spatial aspects. More elaborated model have been developed to describe the nanoheat conduction [15]. The phonon hydrodynamic model [16–19], single- phase-lag model [2] and dual-lag phase model [1] have been applied in modeling thermal transport in nanostructures. Nasri et al. [2, 3] have been investigated the heat transfer in many architecture of nano-MOSFET. They found that the Tri-gate SOI-MOSFET with a wideness of 20 nm is more thermally stable than the device having a length of 10 nm. To study the nature of collision, it is found that the temperature jump boundary condition was an accurate approach to explore the heat transport in interfaces [2]. The ballistic-diffusive equation (BDE) was used to explain the temperature dependence in nano-structure [20, 21]. Humian et al. [22] proposed the BDE to evaluate the heat transport in two-dimensional domain. They have been used the finite element analysis to validate the BDE model. Yang et al. [23] solved the BDE model to access the heat transfer in two-dimensional conventional MOSFET. In this work, we have been developed the BDE model to address the phonon transport in nanodevice. Due to the miniaturization the thermal conductivity, reduce by scattering [24, 25]. The scattering mechanism induced to the use of the ETC [26–29]. We have proposed a theoretical approach, which describe the nature of phonon collision with boundary. The specularly parameter defined as the probability of reflection at boundary [25, 30]. We include this parameter in the ETC to portend the rise of the temperature in nano-structure. To validate our results, the proposed model is tested with results obtained by Yang et al. [23] and a previous work [2, 9]. The proposed (ETC) will be compared with the results obtained by McGaughey et al. [31]. To compute the proposed BDE model depended with the temperature jump boundary condition, we have used the FEM. This method is a useful procedure to model the thermal properties of nanodevice [2].

2. Computer model

The phonon BTE can be defined as [7]:

$$\frac{\partial f(r, v, t)}{\partial t} + v \nabla f(r, v, t) = -\frac{f - f_0}{\tau_R} \quad (2)$$

where f is the distribution function, f_0 is the equilibrium distribution function, v is the group velocity, and τ_R is the relaxation time related to resistive collisions written as

$$\tau_R = \frac{3 \times \kappa}{C \times v^2} \quad (3)$$

where κ is the thermal conductivity written as

$$\kappa = \frac{C \times v \times \Lambda}{3} \quad (4)$$

where Λ is the mean free path defined as $\Lambda = v\tau_R$ and C is the volumetric heat capacity [20]. The ballistic-diffusive approximation is to divide the distribution function into a diffusive term f_m and ballistic term f_b [20]:

$$f = f_m + f_b \quad (5)$$

where f_b arise from the boundary scattering [20], defined as

$$\frac{\partial f_b(r, v, t)}{\partial t} + v \nabla f_b(r, v, t) = -\frac{f_b}{\tau_R} \quad (6)$$

The second part grouped into f_m . The basic equation for f_m is defined as:

$$\frac{\partial f_m(r, v, t)}{\partial t} + v \nabla f_m(r, v, t) = -\frac{f_m - f_0}{\tau_R} \quad (7)$$

We can calculate the diffusive flux [7, 20].

$$q_m(t, r) = \int_{\varepsilon} v(r, t) f_m(r, \varepsilon, t) \varepsilon D(\varepsilon) d\varepsilon \quad (8)$$

where ε is the kinetic energy and $D(\varepsilon)$ is the density of states. By the development in Taylor series to the first order of Eq. (7), we obtain [7]:

$$\tau_R \frac{\partial q_m(r, t)}{\partial t} + q_m(r, t) = -\kappa \nabla T_m(r, t) \quad (9)$$

We use the energy conservation equation to eliminate q_m

$$-\nabla \cdot q(r, t) + \dot{q}_h = \frac{\partial u(r, t)}{\partial t} \quad (10)$$

where \dot{q}_h is the volumetric heat generation, q is the heat flux and u is the internal energy defined as [20].

$$\begin{aligned} q(t, r) &= q_b(t, r) + q_m(t, r) \\ u(t, r) &= u_b(t, r) + u_m(t, r) \end{aligned} \quad (11)$$

We can rewritten two temperature T_b and T_m such that [20, 21].

$$\frac{\partial u}{\partial t} = C \frac{\partial T}{\partial t} = \frac{\partial u_m}{\partial t} + \frac{\partial u_b}{\partial t} = C \left(\frac{\partial T_m}{\partial t} + \frac{\partial T_b}{\partial t} \right) \quad (12)$$

where $T = T_m + T_b$

T_m is the temperature to the diffusive part and T_b arise from the ballistic parts.

By using the same reasoning of Eq. (9), Eq. (6) becomes [20].

$$\tau_R \frac{\partial^2 T_b(r, t)}{\partial t^2} + C \frac{\partial T_b}{\partial t}(r, t) = -\tau_R \times \frac{\partial(\nabla \cdot q_b(r, t))}{\partial t} \quad (13)$$

Substituting Eqs. (9) and (13) into Eq. (10) we obtain the ballistic-diffusive-equation [20, 23].

$$\tau_R \frac{\partial^2 T_m(r, t)}{\partial t^2} + \frac{\partial T_m(r, t)}{\partial t} = \frac{\kappa}{C} \nabla \nabla T_m(r, t) - \frac{\nabla q_m(r, t)}{C} + \frac{\dot{q}_h}{C} + \frac{\tau_R \partial \dot{q}_h}{C \partial t} \quad (14)$$

The conventional Fourier heat conduction equation cannot predict the heat transport in nanostructure. Hua et al. [26] studied the ETC in nanostructure. They derived a model for the ETC based on the phonon BTE written as [26]:

$$\kappa_{eff} = \kappa / (1 + \alpha \times Kn) \quad (15)$$

where $Kn = \frac{\Lambda}{L}$ is the Knudsen number, L is the length of nanofilms and α is a coefficient depend with the geometries.

For $Kn = 0$, Eq. (15) becomes $\kappa_{eff} = \kappa$ (diffusive regime).

For $Kn > 1$, the thermal conductivity reduce due to the ballistic transport. Using the Fourier's law the ETC defined as [26]:

$$\kappa_{eff} = \frac{q \times L}{\Delta T} \quad (16)$$

where L is length of the nanostructure q is the heat flux and ΔT is the temperature difference. Kaiser et al. [28] proposed a non-Fourier heat conduction at the nanoscale. They recently derived an analytic expression for the ETC. In addition, they proved the impact of the temperature jump in nanostructure. In this work, we propose a theoretical model for the ETC [19], defined as

$$k_{eff}(Kn) = \kappa \left[1 - \frac{2Kn \times \tanh(1/2Kn)}{1 + C_W \times \tanh(1/2Kn)} \right] \quad (17)$$

where $C_W = 2 \times \left(\frac{1+p}{1-p} \right)$ is a constant related to the properties of the walls [19] and p is the specularly parameter [30].

For high values of Kn , where the regime ballistic is dominant, the thermal conductivity reduced by scattering (reflection at boundary) [24, 25], Eq. (17) predict that the ETC behaves [19]:

$$\kappa_{eff}(Kn) = \kappa \left(\frac{C_W}{2Kn} \right) \quad (18)$$

In our case, the BDE model rewritten as:

$$\tau_b \frac{\partial^2 T_m(r, t)}{\partial t^2} + \frac{\partial T_m(r, t)}{\partial t} = \frac{\kappa_{eff}}{C} \nabla \nabla T_m(r, t) - \frac{\nabla q_b(r, t)}{C} + \frac{\dot{q}_h}{C} + \frac{\tau_b \partial \dot{q}_h}{C \partial t} \quad (19)$$

where τ_b is the relaxation time related to the phonon scattering at boundary [7] defined as:

$$\tau_b = \frac{3 \times \kappa_{eff}}{C \times v^2} \quad (20)$$

Substituting Eq. (18) into Eq. (20), we obtain the Ziman formula [24]

$$\frac{1}{\tau_b} = \left(\frac{1-p}{1+p} \right) \times \left(\frac{v}{L} \right) \quad (21)$$

where $\frac{1}{\tau_b}$ is the collision rate.

3. Boundary and initial condition

When the ballistic transport appear the temperature jump at boundary occur and cause the reduction of the thermal conductivity [27, 32]. Ben Aissa et al. [12] have been explored a nano-heat conduction in cylindrical surrounding-gate (SG) MOSFET. They used the DPL with the temperature jump applied in the interface oxide-semiconductor defined as

$$\Delta T_{Jump} = -d \times Kn \times L \times \nabla T \quad (22)$$

where d is an adjustable coefficient, the ETC defined as [12]:

$$d = \frac{R \times \kappa_{eff}}{Kn \times L_c} \quad (23)$$

where R is the thermal boundary resistance. The proposed ETC given by Ben Aissa et al. [12, 32] is written as:

$$\kappa_{eff} = \kappa / (1 + (4 \times Kn)) \quad (24)$$

Hua et al. [33, 34] discussed the temperature jump in nanofilms. They have studied the phonon transport in interfaces. They derived a boundary temperature jump defined as

Work	Adjustable coefficient d
Ben Aissa et al. [12]	0.05 For $Kn = 3.33$
Hua and Cao [33]	0.66 For $Kn < 5$
Sing et al. [36]	$\frac{1.25}{Pr}$ For $Kn < 0.1$
Present work	0.09 For $Kn = 10$

Table 1. First-order temperature jump condition.

$$T - T_W = -d \times \Lambda \times \frac{\partial T}{\partial x} \quad (25)$$

where T_W is the temperature jump at the wall.

Yang et al. [35] explained the impact of the temperature jump in the continuum flow and slip flow. They have investigated the heat transfer in nanofluids. At the wall, the temperature jump lead to the following expression by Gad-el-Hak [35]

$$T_S - T_W = \frac{2\beta}{\beta + 1} \frac{2 - \sigma_T}{\sigma_T} \frac{\Lambda}{Pr} \left. \frac{dT}{dy} \right|_{Wall} \quad (26)$$

where T_S is the system temperature and T_W is the wall temperature, σ_T is the thermal accommodation coefficient, β is the ratio of specific heats, and Pr is the gas Prandtl number. Singh et al. [36] noted that in ideal monoatomic gas ($Kn < 0.1$), the temperature jump at the solid interface rewritten as

$$T_S - T_W = \frac{1.25 \times \Lambda}{Pr} \left. \frac{dT}{dy} \right|_{Wall} \quad (27)$$

Due to the utility of the temperature jump, the following expressions are summarized in **Table 1**.

4. Structure to model and numerical method

The architecture used in this present work is the two-dimensional conventional MOSFET. The proposed structure shown in **Figure 1**. The substrate is compound by Silicon (Si). The Si-MOSFETs thickness used in this model is 50 nm. The channel length is $L_c = 10$ nm. In order to compare our results with similar works, the reference temperature is $T_0 = 300$ K and the maximal power generation is $\dot{q}_h = 10^{19} w/m^3$ [23]. The right and left boundaries are assumed to be adiabatic. The temperature jump boundary condition is applied in the interface (Si-SiO₂). In this side the phenomena of collision phonon-wall is more frequent. The MFP used in this proposed work is $\Lambda = 100$ nm [23]. Using Eq. (17), we found that the thermal conductivity reaches $18 \text{ Wm}^{-1} \text{ k}^{-1}$. In this case, the adjustable coefficient d attains 0.09 for $R = 0.503 \text{ K m}^2 \text{ W}^{-1}$ [37].

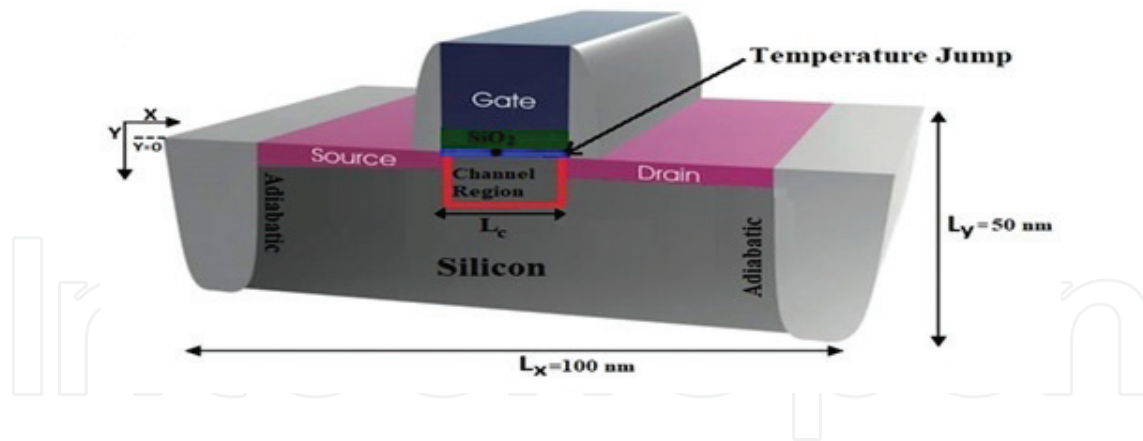


Figure 1. Schematic geometries of the MOSFET transistor.

Symbol	V (m s ⁻¹)	K (Wm ⁻¹ K ⁻¹)	C (J m ⁻³ k ⁻¹)	Λ (nm)	Kn
Si	3000	150	1.5 × 10 ⁶	100	10
SiO ₂	5900	1.4	1.75 × 10 ⁶	0.4	0.04

Table 2. Thermal properties of Silicon and Silicon dioxide.

To solve the BDE model coupled with the temperature jump at boundary we use the FEM [4]. The finite-element approximation used in the BDE model can be defined as:

$$[B]\{T_t\} + [B_1]\{T_{tt}\} - [D]\{T\} = \{m\} \quad (28)$$

where $[B]$, $[B_1]$ and $[D]$ is a matrix valued, $\{T_t\}$, $\{T_{tt}\}$ and $\{T\}$ represent the nodal temperature, $\{m\}$ is the matrix vector.

The discretization of Eq. (25) leads to

$$\{T_{p+1}\} \left(\frac{[B]}{\Delta t} + \frac{[B]}{\Delta t^2} \right) = \{T_p\} \left(\frac{[B]}{\Delta t} + 2 \frac{[B]}{\Delta t^2} + [D] \right) - \{T_{p-1}\} \left(\frac{[B]}{\Delta t^2} \right) + \{m\}_p \quad (29)$$

where Δt is the time step and $\{T_p\}$ is the nodal temperature at the time t_p .

The materials used in our simulation are Silicon [2] and Silicon dioxide [2] and their thermal properties are illustrated in Table 2.

5. Results and discussion

The reduction of the thermal conductivity have a strong dependence with the Knudsen number. We take account the specularly parameter and Knudsen number because we studied the mechanism of boundary scattering.

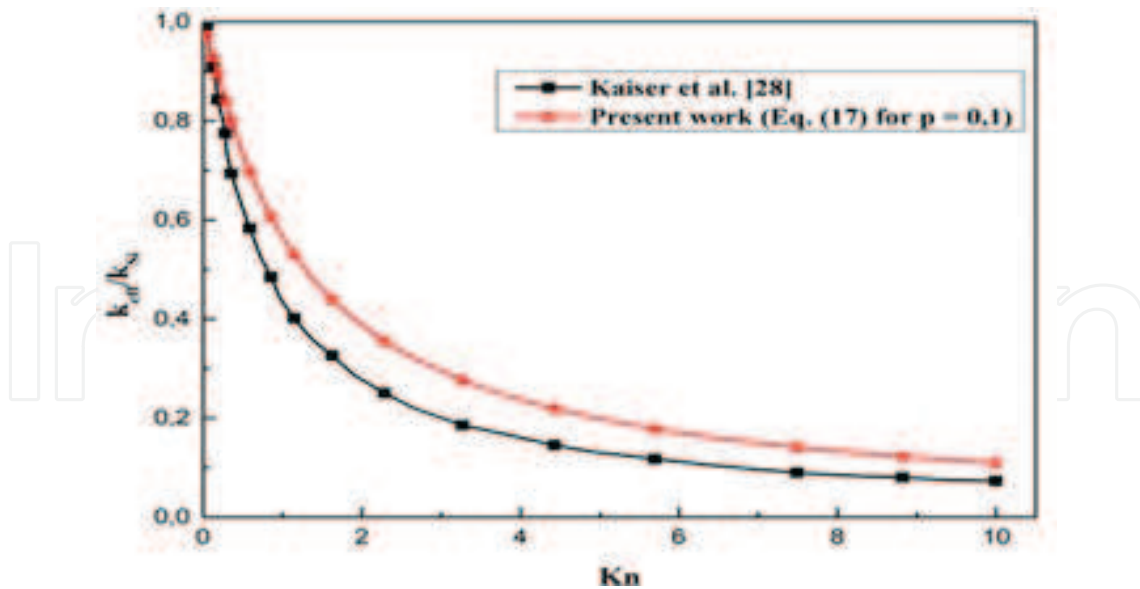


Figure 2. Effective thermal conductivity vs. Knudsen number.

In **Figure 2** we show the impact of the thermal conductivity which depends on the specularity parameter. In this case, we use Eq. (17) to inquire the ETC. It is obvious that the thermal conductivity decreases when the Knudsen number increases. In similarity to the analytical model proposed by Hua and Cao et al. [32], it is found that the thermal conductivity reaches 62% of the bulk value for $Kn = 1$.

Figure 3 plots the ETC for various lengths of nanofilms. For low thin films ($L = 10$ nm) the thermal conductivity attains 10–20% of the bulk value. The ballistic transport involves the rapid increase of the ETC. For $p = 0.25$ we show the same shape obtained by Ma [29]. For thin films ($L > 1000$ nm), $p = 0.25$ is a good approximation.

The advantage of our proposed model is the capture of the increase of the temperature better than the other transport models (DPL, SPL and classical BDE). We associated the BDE model with the temperature jump. The obtained results are presented along the centerline ($L_x/2, Y = 0$) at the time $t = 30$ ps. In the ballistic regime ($Kn = 10$) we use Eq. (18). For high Knudsen numbers, the heat transport is influenced by the mechanism of scattering related to the boundary. This type of collision was examined by Guo et al. [38]; they deduced a discrete-ordinate method (DOM) derived by the Callaway's model [38]. They found acceptable results to determine the ETC in a rectangular graphene ribbon. The Callaway's model is based on a simple boundary scattering.

Figure 4 illustrates the comparison of the peak temperature rise in the nano-transistor at $t = 30$ ps. The classical BDE, BTE, DPL, SPL, Fourier law and our proposed model reach respectively 318.7, 327, 320.5, 318.9, 305 and 322.7 K. The new BDE model captures the increase of the temperature near the BTE. For low thin-film ($L_c = 10$ nm) one can see that the temperature attains the maximum at short time. The saturation of the temperature varied to 12–15 ps for all model transport. The classical Fourier law cannot predict the temperature profile due to the nature of phonon thermal transport [39].

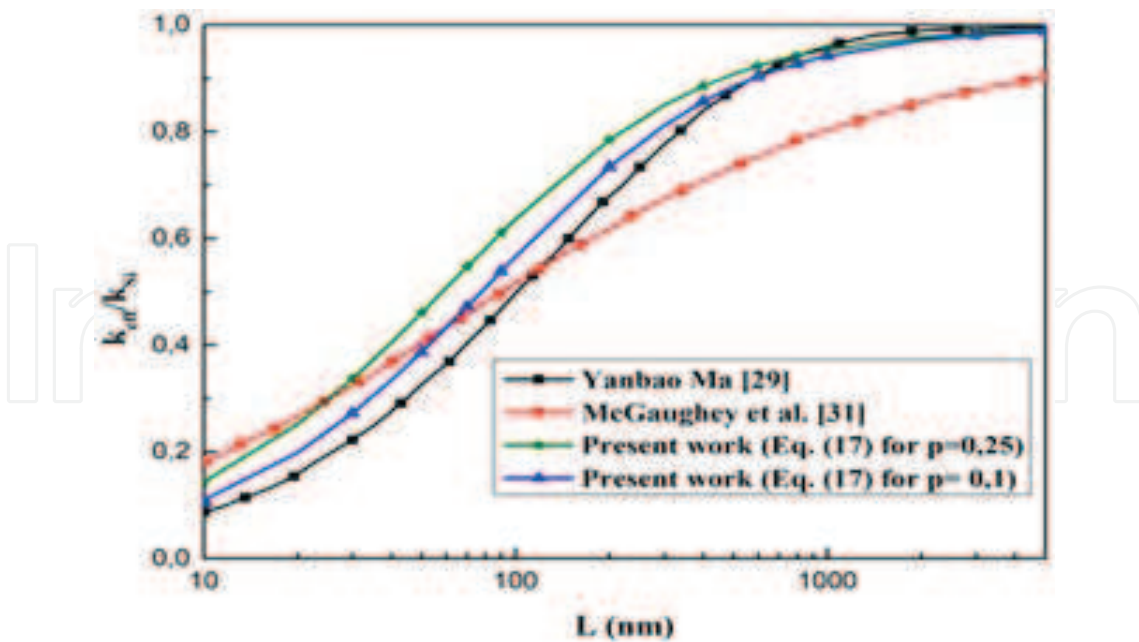


Figure 3. Effective thermal conductivity in Silicon thin film at room temperature.

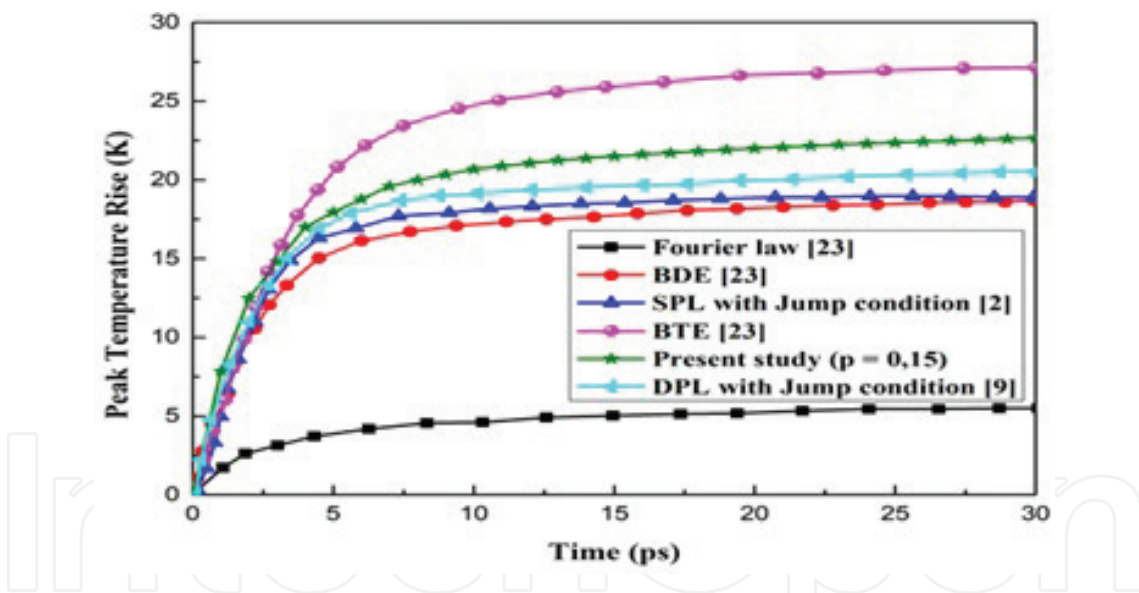


Figure 4. Comparison of the peak temperature at the centerline.

The temperature peak rise in the Y-direction at the centerline of the nanodevice is demonstrated in **Figure 5**. The decrease of the temperature is owned to the reduction of the thermal conductivity. Our present model has the same form with the classical BDE model. The difference appear in low temperature due to the collision rate, which depend on the specularity.

Figure 6 illustrate the 2D distribution of the temperature at $t = 30$ ps. In a short time, the temperature increase in the left and right side of the channel region. This side known as the heat zone of the nanodevice. A self-heating processes appear due to nature of the phonon

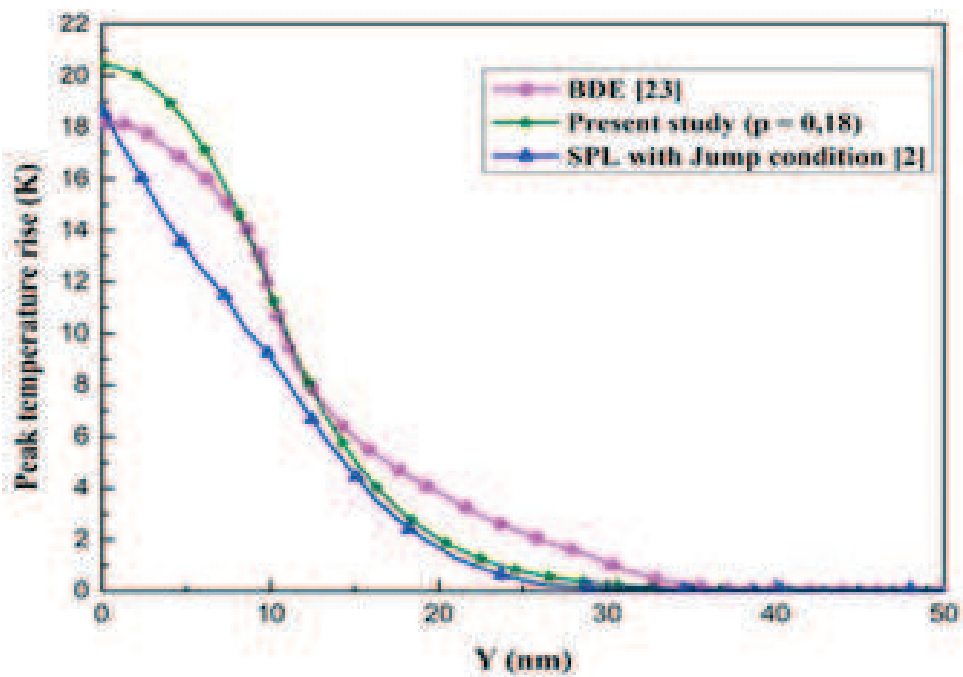


Figure 5. Peak temperature rise versus Y-axis at the centerline of the MOSFET at t = 10 ps.

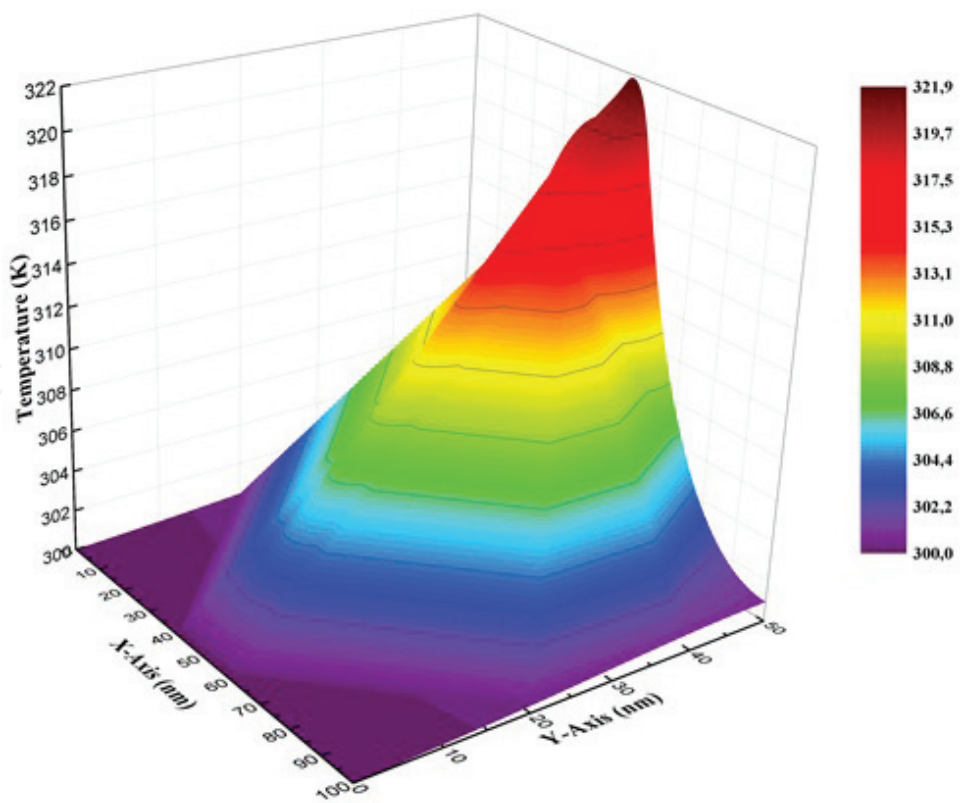


Figure 6. A 2D temperature distribution for p = 0.18 at t = 30 ps.

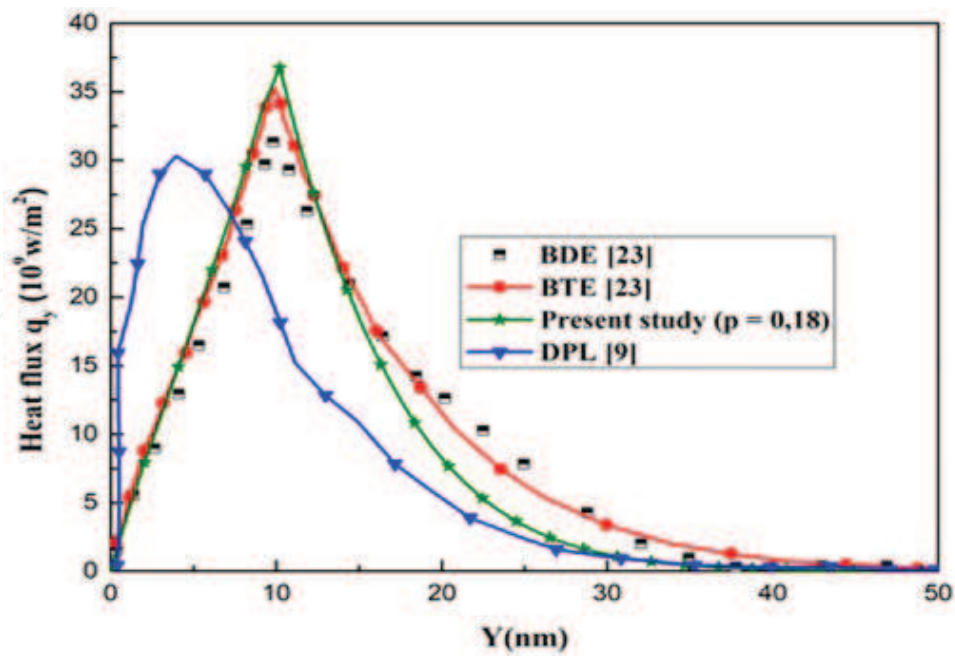


Figure 7. Comparison of the heat flux in the Y direction at $t = 10$ ps.

collision which is characterized by a frequent scattering at boundary. The augmentation of the temperature cause an important dissipation of energy, which affect the environment. In the last years, organic electronic was made to reduce the energy consumption and the thermal resistance between materials [40].

Figure 7 shows the comparison of the heat flux in the Y-direction at the centerline of nano-MOSFET. Using the BDE model for $p = 0.18$, we obtain the same shape and amplitude given by the BTE. The temperature jump at boundary is a good argument to predict the non-Fourier heat transfer [41]. The increase of the heat flux is caused by two reason: the reduction of the thermal conductivity and the length of nanostructure. To reduce the heat dissipation in nanoelectronic materials, it is necessary that the current densities was minimized [9]. A preferment devise is characterized by minimal power consumption. In a technological concept, the graphene is an excellent material which described by high thermal conductivity and low temperature rise [25, 42].

6. Conclusions

In this chapter, we report a nano-heat conduction based on the BDE model. The temperature jump is good proof to study the thermal properties of nano-materials. Our proposed model is efficient approach for the non-Fourier heat conduction. In addition, our obtained results agree with other transport model. In nanostructure the reduction of the thermal conductivity and phonon collision mechanism. Our study explain the distribution of the temperature in 10 nm

MOSFET. The maximal temperature is located in the interface oxide-semiconductor. To reduce the effect of the thermal transport in nano-electronic materials it is obvious that we should replace Si based materials by organic technologies (carbon based). Green electronics are involved in recent integrated circuits, solar cell and high-speed processors. In addition, green materials has a wide biocompatibility and a safe impact on the environment [43].

Author details

Housseem Rezgui, Faouzi Nasri*, Mohamed Fadhel Ben Aissa and Amen Allah Guizani

*Address all correspondence to: nasrifaouzi90@yahoo.fr

Laboratory of Thermal Processes, Research and Technology Centre of Energy, Hammam-Lif, Tunisia

References

- [1] Nasri F, Ben Aissa MF, Belmabrouk H. Effect of second-order temperature jump in metal-oxide-semiconductor field effect transistor with dual-phase-lag model. *Microelectronics Journal*. 2015;**46**(1):67-74
- [2] Nasri F, Ben Aissa MF, Gazzah MH, Belmabrouk H. 3D thermal conduction in nanoscale tri-gate MOSFET based on single-phase-lag model. *Applied Thermal Engineering*. 2015; **91**:647-653
- [3] Nasri F, Ben Aissa MF, Belmabrouk H. Microscale thermal conduction based on Cattaneo-Vernotte model in silicon on insulator and double gate MOSFETs. *Applied Thermal Engineering*. 2015;**76**:206-211
- [4] Fiori G, Bonaccorso F, Iannaccone G, Palacios T, Neumaier D, Seabaugh A, Banerjee S, Colombo L. Electronic based on two-dimensional materials. *Nature Nanotechnology*. 2014;**9**. DOI: 10.1038/NNANO.2014.207
- [5] Dong Y, Cao BY, Guo ZY. Thermomass theory: A mechanical pathway to analyse anomalous heat conduction in nanomaterials. In: Vakhrushev A, editor. *Nanomechanics*. Rijeka: InTech; 2017. DOI: 10.5772/67780
- [6] Xu M, Li X. The modeling of nanoscale heat conduction by Boltzmann transport equation. *International Journal of Heat and Mass Transfer*. 2012;**55**:1905-1910
- [7] Xu M, Hu H. A ballistic-diffusive heat conduction model extracted from Boltzmann transport equation. *Proceedings of the Royal Society A*. 2011;**467**:1851-1864
- [8] Pisipati S, Chen C, Geer J, Sammakia B, Murray BT. Multiscale thermal device modeling using diffusion in the Boltzmann transport equation. *International Journal of Heat and Mass Transfer*. 2013;**64**:286-303

- [9] Nasri F, Echouchene F, Ben Aissa MF, Graur I, Belmabrouk H. Investigation of Self-heating effects in a 10-nm SOI-MOSFET with an insulator region using electrothermal modeling. *IEEE (Institute of Electrical and Electronics Engineers) Transaction on Electron Devices*. 2015;**62**:2410-2415
- [10] Nasri F, Ben Aissa MF, Belmabrouk H. Nanoheat conduction performance of black phosphorus field-effect transistor. *IEEE (Institute of Electrical and Electronics Engineers) Transaction on Electron Devices*. 2017;**64**:2765-2769
- [11] Nasri F, Ben Aissa MF, Belmabrouk H. Nonlinear electrothermal model for investigation of heat transfer process in a 22-nm FD-SOI MOSFET. *IEEE (Institute of Electrical and Electronics Engineers) Transaction on Electron Devices*. 2017;**4**:1461-1466
- [12] Ben Aissa MF, Nasri F, Belmabrouk H. Multidimensional nano heat conduction in cylindrical transistors. *IEEE (Institute of Electrical and Electronics Engineers) Transaction on Electron Devices*. 2017;**64**:5236-5241
- [13] Wang HD, Cao BY, Guo ZY. Heat flow in carbon nanotubes. *International Journal of Heat and Mass Transfer*. 2010;**53**:1796-1800
- [14] Alvarez FX, Jou D. Memory and nonlocal effects in heat transport: From diffusive to ballistic regimes. *Applied Physics Letters*. 2007;**90**:083109
- [15] Tzou DY. *Macro-to Microscale Heat Transfer: The Lagging Behavior*. Chichester: John Wiley & Sons; 2014
- [16] Alvarez FX, Jou D, Sellitto A. Phonon hydrodynamics and phonon-boundary scattering in nanosystems. *Journal of Applied Physics*. 2009;**105**(1):014317
- [17] Jou D, Criado-Sancho M, Casas-Vázquez J. Heat fluctuations and phonon hydrodynamics in nanowires. *Journal of Applied Physics*. 2010;**107**(8):084308
- [18] Guo Y, Wang M. Phonon hydrodynamics for nanoscale heat transport at ordinary temperatures. *Physical Review B*. 2018;**97**(3):035421
- [19] Sellitto A, Carlomango I, Jou D. Two-dimensional phonon hydrodynamics in narrow strips. *Proceedings of the Royal Society A*. 2015;**471**:20150376
- [20] Chen G. Ballistic-diffusive heat-conduction equations. *Physical Review Letters*. 2001;**86**:2297-2300
- [21] Chen G. Ballistic-diffusive equations for transient heat conduction from nano to macroscales. *ASME (The American Society of Mechanical Engineers) Journal Heat Transfer*. 2002;**124**:320-328. DOI: 10.115/1.1447938
- [22] Hamian S, Yamada T, Faghri M, Park K. Finite element analysis of transient ballistic-diffusive phonon heat transport in two-dimensional domains. *International Journal of Heat and Mass Transfer*. 2015;**80**:781-788
- [23] Yang R, Chen G, Laroche M, Taur Y. Simulation of nanoscale multidimensional transient heat conduction problems using ballistic-diffusive equations and phonon Boltzmann

- equation. ASME (The American Society of Mechanical Engineers) Journal Heat Transfer. 2005;**127**:298-306
- [24] Ghosh S, Bao W, Nika DL, Subrina S, Pokatilov EP, Lau CN, Balandin AA. Dimensional crossover of thermal transport in few-layer graphene. *Nature Materials*. 2010;**9**:555-558
- [25] Balandin AA. Thermal properties of graphene and nanostructured carbon materials. *Nature Materials*. 2011;**10**:569-581
- [26] Hua YC, Cao BY. An efficient two-step Monte Carlo method for heat conduction in nanostructures. *Journal of Computational Physics*. 2017;**342**:253-266
- [27] Sobolev SL. Discrete space-time model for heat conduction: Application to size dependent thermal conductivity in nano-films. *International Journal of Heat and Mass Transfer*. 2017;**108**:933-939
- [28] Kaiser J, Feng T, Maassen J, Wang X, Ruan X, Lundstrom M. Thermal transport at the nanoscale: A Fourier's law vs. phonon Boltzmann equation study. *Journal of Applied Physics*. 2017;**121**:044302. DOI: 10.1063/1.4974872
- [29] Ma Y. Size-dependent thermal conductivity in nanosystems based on non-Fourier heat transfer. *Applied Physical Letters*. 2012;**101**(21):211905
- [30] Ziman JM. *Electrons and Phonons: The Theory of Transport Phenomena in Solids*. Oxford: Oxford University Press; 2001
- [31] McGaughey AJ, Landry ES, Sellan DP, Amon CH. Size-dependent model for thin film and nanowire thermal conductivity. *Applied Physical Letters*. 2011;**99**(13):131904
- [32] Hua YC, Cao BY. The effective thermal conductivity of ballistic-diffusive heat conduction in nanostructures with internal heat source. *International Journal of Heat and Mass Transfer*. 2016;**92**:995-1003
- [33] Hua YC, Cao BY. Slip boundary conditions in ballistic-diffusive heat transport in nanostructures. *Nanoscale and Microscale Thermophysical Engineering*. 2017;**21**(3):159-176
- [34] Hua YC, Cao BY. Phonon ballistic-diffusive heat conduction in silicon nanofilms by Monte Carlo simulations. *International Journal of Heat and Mass Transfer*. 2014;**78**:755-759
- [35] Yang C, Wang Q, Nakayama A, Qiu T. Effect of temperature jump on forced convective transport of nanofluids in the continuum flow and slip flows regimes. *Chemical Engineering Science*. 2015;**137**:730-739
- [36] Singh D, Guo X, Alexeenko A, Murthy JY, Fisher TS. Modeling of subcontinuum thermal transport across semiconductor-gas interfaces. *Journal of Applied Physics*. 2009;**106**:024314
- [37] Mahajan SS, Subbarayan G. Estimating Kapitza resistance between Si-SiO₂ Interface using molecular dynamics simulations. *IEEE (Institute of Electrical and Electronics Engineers) Transactions on components, Packaging and Manufacturing Technology*. 2011;**1**(8):1132-1139

- [38] Guo Y, Wang M. Heat transport in two-dimensional materials by directly solving the phonon Boltzmann equation under Callaway's dual relaxation model. *Physical Review B*. 2017;**96**:134312
- [39] Nie BD, Cao BY. Reflection and refraction of a thermal wave at an ideal interface. *International Journal of Heat and Mass Transfer*. 2018;**116**:314-328
- [40] Irimia-Vladu M. Green electronics: Biodegradable and biocompatible materials and devices for sustainable future. The Royal Society of Chemistry. 2014;**43**:588-610. DOI: 10.1039/c3cs60235d
- [41] Criado-Sancho M, Jou D. A simple model of thermoelastic heat switches and heat transistors. *Journal of Applied Physics*. 2017;**121**:024503. DOI: 10.1063/1.4974011
- [42] Pop E, Varshney V, Roy AK. Thermal properties of graphene: Fundamentals and applications. *MRS Bulletin*. 2012;**37**:1273-1281. DOI: 10.1557/mrs.2012.203
- [43] Irimia-Vladu M, Glowacki E, Voss G, Bauer S, Sariciftci NS. Green and biodegradable electronics. *Materials Today*. 2012;**15**:340-346. DOI: 10.1016/S1369-7021(12)70139-6

IntechOpen

